Circulation

ORIGINAL RESEARCH ARTICLE

Comprehensive Ex Vivo Comparison of 5 Clinically Used Conduit Configurations for Valve-Sparing Aortic Root Replacement Using a 3-Dimensional–Printed Heart Simulator

BACKGROUND: Many graft configurations are clinically used for valve-sparing aortic root replacement, some specifically focused on recapitulating neosinus geometry. However, the specific impact of such neosinuses on valvular and root biomechanics and the potential influence on long-term durability are unknown.

METHODS: Using a custom 3-dimenstional–printed heart simulator with porcine aortic roots (n=5), the anticommissural plication, Stanford modification, straight graft (SG), Uni-Graft, and Valsalva graft configurations were tested in series using an incomplete counterbalanced measures design, with the native root as a control, to mitigate ordering effects. Hemodynamic and videometric data were analyzed using linear models with conduit as the fixed effect of interest and valve as a fixed nuisance effect with post hoc pairwise testing using Tukey's correction.

RESULTS: Hemodynamics were clinically similar between grafts and control aortic roots. Regurgitant fraction varied between grafts, with SG and Uni-Graft groups having the lowest regurgitant fractions and anticommissural plication having the highest. Root distensibility was significantly lower in SG versus both control roots and all other grafts aside from the Stanford modification ($P \leq 0.01$ for each). All grafts except SG had significantly higher cusp opening velocities versus native roots ($P<0.01$ for each). Relative cusp opening forces were similar between SG, Uni-Graft, and control groups, whereas anticommissural plication, Stanford modification, and Valsalva grafts had significantly higher opening forces versus controls ($P<0.01$). Cusp closing velocities were similar between native roots and the SG group, and were significantly lower than observed in the other conduits ($P \leq 0.01$ for each). Only SG and Uni-Graft groups experienced relative cusp closing forces approaching that of the native root, whereas relative forces were >5-fold higher in the anticommissural plication, Stanford modification, and Valsalva graft groups.

CONCLUSIONS: In this ex vivo modeling system, clinically used valve-sparing aortic root replacement conduit configurations have comparable hemodynamics but differ in biomechanical performance, with the straight graft most closely recapitulating native aortic root biomechanics.

Michael J. Paulsen, MD
Annabel M. Imbrie-Moore, MS
Michael Baiocchi, PhD
Hanjay Wang, MD
Camille E. Hironaka, BS
Haley J. Lucian, BS
Justin M. Farry, BSE
Akshara D. Thakore, MS
Yuanjia Zhu, MD
Michael Ma, MD
John W. MacArthur Jr, MD
Y. Joseph Woo, MD

Key Words: aorta ■ aortic aneurysm ■ aortic root ■ aortic valve ■ biomechanics ■ sinus of valsalva ■ surgery

Sources of Funding, see page 1372

https://www.ahajournals.org/journal/circ

ORIGINAL RESEARCH ARTICLE

Clinical Perspective

What Is New?

- Many grafts are available for use in valve-sparing aortic root replacement, some specifically focused on recreating sinus of Valsalva geometry; however, the specific impact of such neosinuses on valvular and root biomechanics and the potential influence on long-term durability are unknown.
- This study presents a comprehensive ex vivo biomechanical study of all available grafts using a novel 3-dimensional–printed left heart simulator and an incomplete counterbalanced repeated measures design with native roots as their own controls to mitigate bias.

What Are the Clinical Implications?

- Neosinus recreation does not appear to result in more normal biomechanical parameters, and the grafts that recreated neosinuses universally experienced higher cusp opening and closing velocities.
- Like the other neosinus grafts, the novel Uni-Graft sinus graft experienced higher cusp opening and closing velocities; however, its unique design mitigated cusp forces with lower forces than other neosinus grafts.
- Contrary to intuition, the straight graft without neosinuses results in the lowest cusp opening and closing velocities and forces of all grafts tested.
- Lower cusp forces likely have long-term implications and may explain differences in durability seen clinically.

The treatment of aortic root aneurysms was revolutionized by the development of valve-sparing aortic root replacement using the reimplantation and remodeling operations.[1,2] Before the implementation of these valve-sparing strategies, patients with an aortic root aneurysm and a normal aortic valve underwent root replacement with either a mechanical valve necessitating lifelong anticoagulation or a bioprosthetic valve with the risk of structural deterioration requiring future reoperation, which in young patients is all but certain. Although both the remodeling and reimplantation operations spare the aortic valve, the remodeling technique alone does not address or prevent further annular dilation, although the addition of an annuloplasty ring may be effective.[3] Some studies have suggested that the remodeling technique, which also spares the shape of the sinuses of Valsalva, results in more natural aortic root biomechanics.[4,5] However, reimplantation of the aortic valve addresses annular dilation and externally supports any remaining abnormal valvular tissue, and in some series, demonstrates greater long-term durability.[6–8]

Several modifications to the reimplantation technique have been described in both the graft used and operation performed, with the primary focus on recreating the sinuses of Valsalva, as many studies demonstrate that these structures play an important role in maintaining optimal biomechanics and fluid dynamics within the aortic root.[9–16] This is highly intuitive, yet Dr. Tirone David observed greater long-term durability with the straight graft (SG) compared with grafts with neosinuses. Others have found similar results comparing SGs with Valsalva grafts (VGs).[17] To elucidate why this may be occurring, we investigated these 2 conduits using an ex vivo heart simulator and found that, contrary to theory and even some 4-dimensional magnetic resonance imaging studies, the addition of neosinuses with the VG results in higher leaflet velocities and forces.[18] Based on our observations and the data we collected, we attributed the higher velocities and forces to radial, spherical displacement of the commissures in the VG. However, multiple additional conduits and modifications exist. These include the anticommissural plication (ACP) technique, which uses a specific formula for graft sizing based on cusp height, tending to oversize the graft versus the straight conduit, but then plicating the graft between the commissures at the nadir of each sinus at both the annular level and the sinotubular junction to recreate neosinuses.[19] In addition, the ACP technique alters the normally planar annular suture line and uses an accentuated coronet-shaped suture line, which, together with the oversized graft, results in much larger neosinuses than other methods, such as the David V technique, which also plicates a mildly oversized graft between the commissures, which is posited to be the reason that these other methods do not sufficiently restore normal cusp stresses.[15,20,21] The Stanford modification (Sm) is another variation on the David V technique that uses a graft that is oversized by 6 to 8 mm based on the original David–Feindel formula. However, rather than plication, the proximal end of the graft is necked down over an appropriately sized valve sizer with approximately 10 interrupted sutures.[22] The larger graft is then trimmed to the level of the top of the commissures and anastomosed to a smaller graft over the valve sizer to recreate the sinotubular junction.[22]

Completely novel graft designs have also been described and produced commercially in addition to the VG. One of the more recent innovations is the Uni-Graft W SINUS (UG) prosthesis, manufactured in Germany.[23] The UG is an anatomically correct woven Dacron graft that maintains the commissures in their native cylindrical position, but also possesses sinuses woven directly into the graft. Preliminary studies have been encouraging with reportedly near-normal geometry and hemodynamics.[23,24] In this study, we expanded on our previous biomechanical engineering research and compared the performance of not only the straight and VGs but

also the UG, the Sm, and the ACP technique with the native aortic root serving as the control utilizing a counterbalanced crossover design.

METHODS

Experimental Design

The data that support the findings of this article are available from the corresponding author on reasonable request. Building on our previous work in which we studied the biomechanical differences between SGs and VGs utilizing a 3-dimensional–printed ex vivo left heart simulator,[18] we sought to perform a reliable comparison between five of the most commonly used modifications and graft options, which include, in addition to straight and VGs,[25,26] the UG,[23] the Sm of the David V technique,[22,27,28] and the ACP technique (Figure 1A).[19] To eliminate potential error from using a different valve to test each graft individually, we used a repeated measures crossover, whereby each valve within its native aortic root serves as its own control, and is then reimplanted into each graft variation sequentially. Five separate, anatomically normal, and similarly sized porcine aortic roots (n=5) were used in this study, with each native aortic root first being mounted into the simulator for baseline control data to be gathered before any reimplantation procedures were performed. The porcine hearts and aortas were obtained from a local abattoir in accordance with institutional guidelines. Next, each of the 5 porcine roots was reimplanted into each of the 5 experimental conduit groups in the specific sequence described below for a total of 6 identical conditions being tested per valve (5 experimental graft conditions and 1 control condition). All of the reimplantation procedures were performed by the same surgeon. Because repeated operations and testing on a single, unfixed (and decomposing) porcine valve has, to at least some degree, detrimental effects on performance, we must account for these sources of bias. To mitigate this error because of order effects, we used an incomplete counterbalanced design where graft sequence is predetermined in a 5×5 matrix to allow each graft to serve 1 time as the first, second, third, fourth, and final operation performed on a particular valve while still testing each experimental condition on every valve (Figure 1B).

Graft Preparation

Five conduit grafts were prepared meticulously to ensure identical relative dimensions to one another in terms of annular height above the proximal end of the graft, coronary ostia position and height, sinotubular junction height, and overall length. For all grafts, the overall length was 50 mm, and the surgical annulus (basal ring) was to be 10 mm above the proximal end of the conduit. Coronary ostia were 5 mm in diameter and placed centrally within the sinus at a height of 14 mm above the annular line. In the VG and UG, this corresponded to a distance in the middle of the neosinus. Silicone tubing with a 4-mm internal diameter and 6-mm external diameter was anastomosed to the grafts in an end-to-side fashion, which could be used to connect the grafts to the mock coronary circulation (described in more detail in the following section). For the SG, a size 28-mm Dacron conduit was used (Gelweave, Vascutek Terumo, Renfrewshire, Scotland). A size 28 VG (Vascutek Terumo) and size 28 UG (Uni-Graft W SINUS, Braun, Melsungen, Germany) were similarly used. To prepare the Sm graft, a 34-mm tubular graft 38 mm in length was anastomosed to a 28-mm tubular graft approximately 12 mm in length with 4-0 polypropylene suture in continuous running fashion. The proximal end was necked down over a size 29 aortic valve sizer as described in the literature.[22] For the ACP graft, a size 34 graft was also used as recommended by the formula accompanying the description of this modification based on the anatomic sizes of the porcine valves we selected (as described in the following section), and the graft was plicated proximally and distally between the commissures at the recommended heights.[19]

Modified Aortic Root Mount and Sample Preparation

To perform multiple operations on a single valve, and to more closely model the native left ventricular outflow tract, we modified our model aortic root and coronary circulation used previously.[18] Rather than sewing the valve entirely within the conduit, including the proximal left ventricular outflow tract (LVOT), and then mounting the conduit and valve within our aortic root mount, we created a 2-part lower root mount consisting of (1) a rigid base with a 28-mm internal diameter central bore and embedded coronary flow channels, and (2) a 28-mm internal diameter elastomeric sewing ring (Figure 2A). Porcine aortic roots were carefully selected to be as close to identical in size and dimensions as possible, with average native cusp height of 17.0±0.7 mm, average native commissural height of 22.4±0.4 mm, and annular diameters of 27.0±1.4 mm. The roots with attached coronaries were dissected free and separated from the heart, leaving an approximately 5-mm cuff of LVOT below the aortic annulus. With the combination of this elastomeric portion of the conduit mount in addition to the cuff of LVOT tissue left on the samples, we aimed to preserve the natural movement of the LVOT during the cardiac cycle. However, in our model, it is passive movement and does not fully mimic the dynamic motion of the LVOT as seen in vivo. The detached roots were preserved in normal saline; no fixative was used. The cuff of left ventricular muscle was sewn to the elastomeric portion of the root mount with a 2-0 running polypropylene suture reinforced with a thin strip of polytetrafluoroethylene tissue patch serving as a circumferential pledget to reinforce the devitalized tissue through multiple tests (Figure 2B and 2C). Although the aortic wall, annulus, and leaflet tissues maintain integrity during testing, the muscular LVOT is prone to more rapid decomposition without preservation, hence the reinforcement. To prolong tissue integrity, the roots and attached conduit mounts were vacuum-sealed in a volume of normal saline and refrigerated at 4°C between trials, and the experiments on each valve were completed sequentially within as short a period of time as possible, typically within 3 days for completion of all tests with a maximum cutoff of 7 days. For tests of the native aortic root, the ascending aorta was trimmed to fit within our aortic root mount (approximately 50 mm in length) and attached to the top conduit mount piece with heavy braided nylon suture. The coronaries were secured to flexible tubes leading into the coronary flow channels, which were then exteriorized through the pump and passed through a dual mock coronary flow circulation described in more detail

A

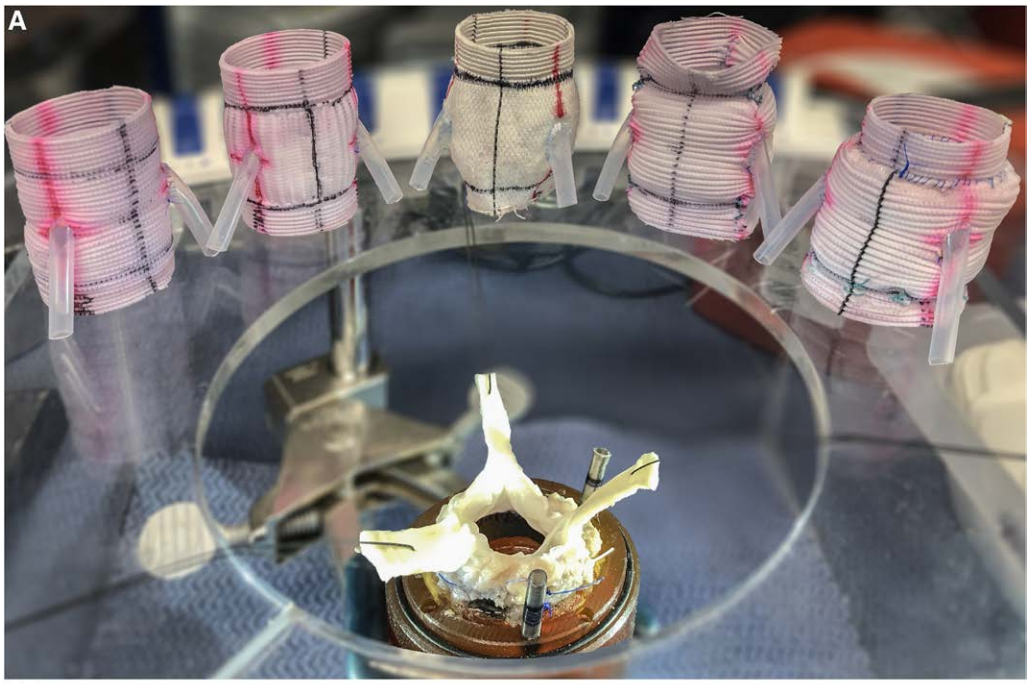

B

Sequence \ Valve	Valve 1	Valve 2	Valve 3	Valve 4	Valve 5
Control	Control	Control	Control	Control	Control
Operation 1	Straight	S-mod	AC Plication	Valsalva	Uni-Graft
Operation 2	Uni-Graft	Straight	S-mod	AC Plication	Valsalva
Operation 3	Valsalva	Uni-Graft	Straight	S-mod	AC Plication
Operation 4	AC Plication	Valsalva	Uni-Graft	Straight	S-mod
Operation 5	S-mod	AC Plication	Valsalva	Uni-Graft	Straight

Figure 1. Experimental setup and design.
A, Optimized model aortic root with each of the grafts to be tested, from left to right: straight graft, Valsalva graft, Uni-Graft, graft with anticommissural plication (AC plication), and graft with the Stanford modification (S-mod). **B**, Incomplete counterbalanced crossover study design.

in the following section. After testing and data collection (as described below), the aortic root (which remained attached to the root mount proximally) was trimmed and reimplanted into each graft using the reimplantation technique with 9 interrupted 2-0 braided polyester unpledgeted horizontal mattress sutures used for the annular suture line. For the second suture line, we used 4-0 polypropylene suture (Figure 3).

Left Heart Simulator

To perform an in-depth study of the biomechanical parameters—including hemodynamics, graft compliance, and leaflet kinematics, among other factors—of the aortic valve within the various conduits, we used our ex vivo left heart simulator, which has been comprehensively described previously (Figure 4A and 4B).[18,29–33] Briefly, the system is comprised of a modular 3-dimensional–printed (Carbon M2, Carbon 3D Inc., Redwood City, CA) and machined enclosure mounted to a pulsatile linear actuator (Superpump, Vivitro Labs, Vancouver, Canada). The enclosure consists of a main ventricular chamber attached to the piston with a left atrial chamber with venous reservoir, and an aortic outflow assembly that connects in a complete circuit through a series of compliance chambers, flow meters, a heat exchanger, and a peripheral resistance valve. In the mitral position, a leakless 28-mm disc valve (Vivitro) was used, which was secured within a 3-dimensional–printed elastomeric gasket and clamped between the left atrium and left ventricular chambers. The system also contains a viscoelastic impedance adaptor that serves to reduce noise artifact and produce more physiological waveforms. The pump was tuned to generate an effective stroke volume of 70 mL at 70 beats per minute, producing a cardiac output of 5 liters per minute. A ventricular waveform complying with ISO 5840 standards for in vitro valve testing was used. Our reference valve was a 29 mm St. Jude mechanical valve, and these parameters were kept constant for all tests. As mentioned, the coronary blood flow passed via channels embedded within the conduit mount, which were exteriorized through the chamber wall, and then routed through a dual mock coronary circuit with differential variable resistance achieved by routing a segment of the left coronary circuit through the ventricular chamber with thin-walled silicone tubing to mimic the resistance of ventricular contraction, followed by a series of compliance elements, electromagnetic flow meters, and throttle valves, before passing back into the venous reservoir (Figure 4C). The coronary circulation was also calibrated

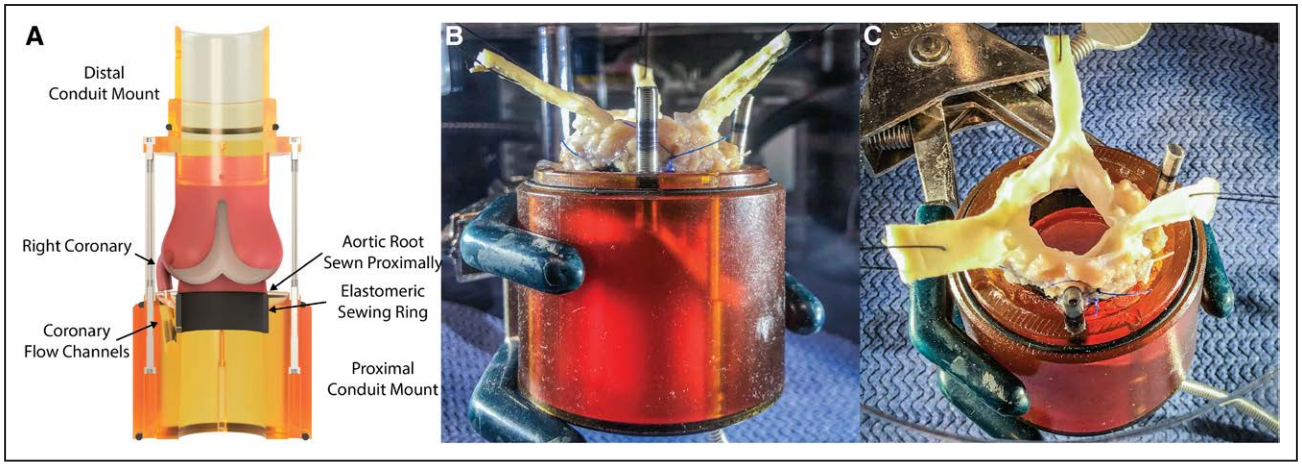

Figure 2. Valve-sparing root model.
A, Schematic of optimized model aortic root in cross-section with labeled components. **B**, Side view of native porcine aortic root after control test has been performed, now prepared for valve-sparing root replacement with reimplantation into the first experimental graft. **C**, View from above of native porcine root sewn into aortic root mounting device.

with the aforementioned reference valve to generate flows of approximately 250 mL/min. For each test valve, the pump was calibrated with the native aortic root to generate a mean arterial pressure of 100 mm Hg, with systolic of 120 mm Hg and diastolic of 80 mm Hg, and with cardiac output of 5 liters per minute. To obtain these parameters, adjustments in compliance and resistance were made, which were noted and kept constant for all experimental trials within that valve.

Data Collection and Statistical Analysis

Our testing platform has the capability to collect an assortment of data, including pressure waveforms in each chamber of the heart, as well as highly accurate flow integrations using 2 electromagnetic flow meters, 1 near the mitral position and 1 near the aortic position. The chamber has view ports and mounting brackets for a high-speed camera system capable of recording at

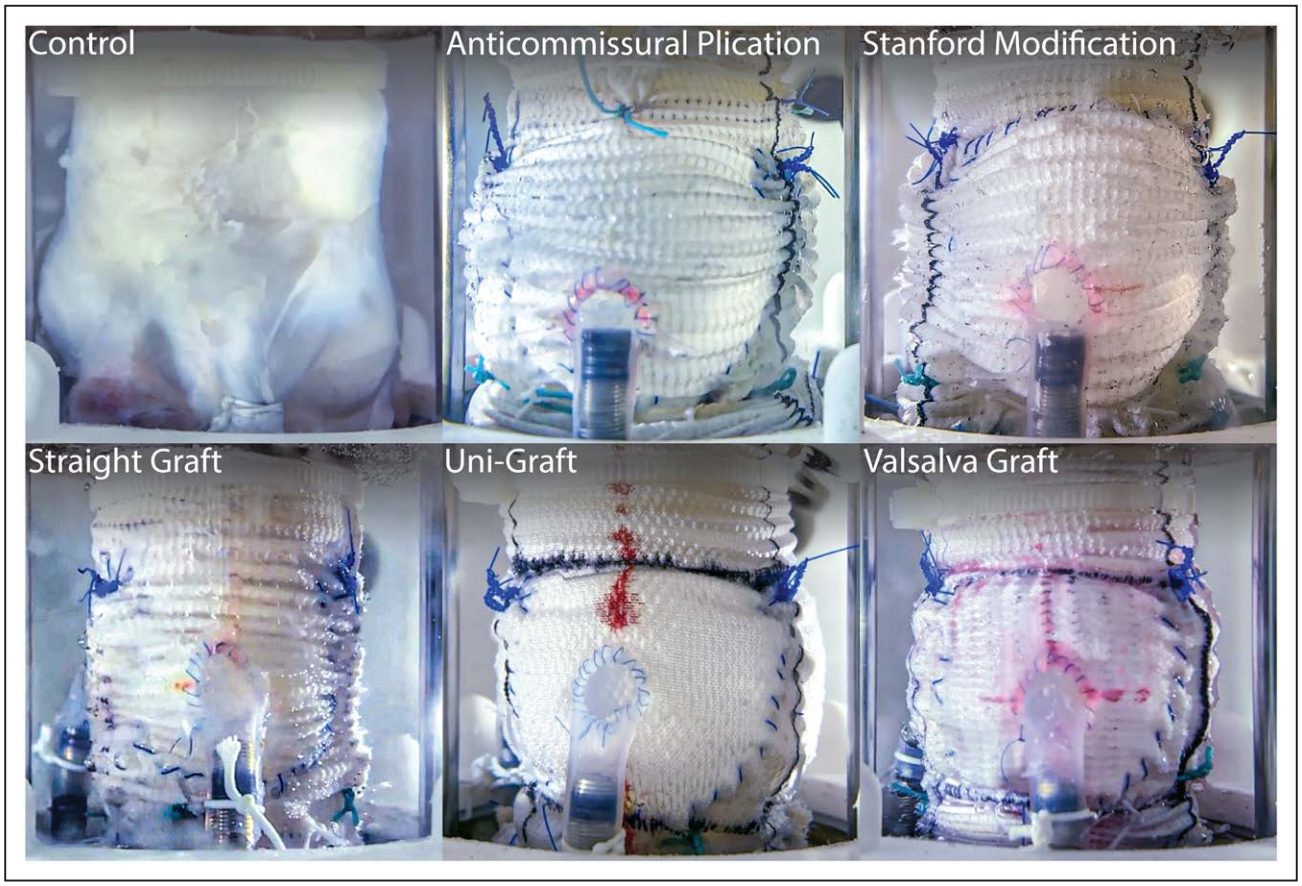

Figure 3. Side-view of experimental conduits tested.
Side profile view of each conduit type mounted within the left heart simulator and attached to the coronary circulation.

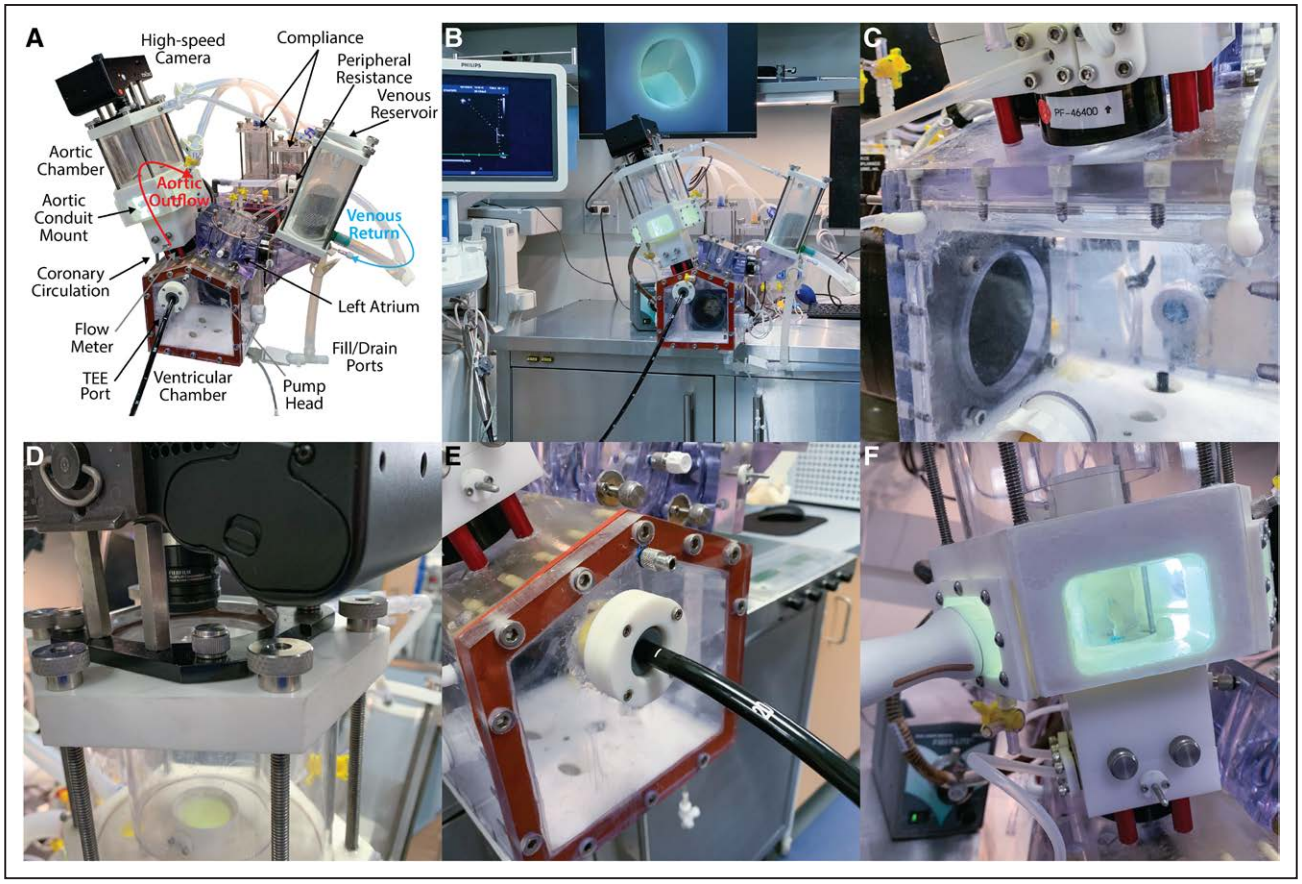

Figure 4. Components of the Stanford left heart simulator system.
A, Left heart simulator labeled component drawing. **B**, Overview of the entire experimental setup, including the left heart simulator, echocardiography machine, and high-speed videometric output. Computers, flow meters, pump controllers, input/output controller, and data acquisition system are in the cabinet below and not shown. **C**, Close-up view of the dual differential-resistance coronary circulation with intraventricular left coronary segment replicating physiological conditions. **D**, High-speed camera mounted to the top of the aortic root and aortic assembly. **E**, View of transesophageal echocardiography (TEE) port within the left ventricular chamber for analysis. **F**, Transthoracic echocardiography port on the side of the aortic root enclosure for obtaining accurate in-plane images of the cusps.

over 1000 frames per second (Chronos 1.4, Kron Technologies, Burnaby, Canada), installed for consistent, clear, and calibrated high-speed videometric analyses from the top and side views (Figure 4D). A port for a transesophageal echo probe (X5-2T, Philips) has been built into the ventricular chamber to obtain apical views for pulsed wave and continuous wave Doppler measurements (Figure 4E). The aortic root compliance assembly has a unique hexagonal configuration with soft windows to allow for excellent transverse views of the valve using a transthoracic probe (S5-1, Philips) for M-mode leaflet velocity measurements, as well as 2-dimensional B-mode with color Doppler to assess for regurgitation (Figure 4F). The coronary circulation is equipped with pressure and flow measurement capabilities to assess coronary mass flow rate and pressure. Raw data were imported into MATLAB (R2019a, MathWorks Inc., Natick, MA) for signal processing, composite plotting, and summary data generation. Summary data were imported into R for statistical analysis (R 4.0.24.0.2). We used linear models to analyze the incomplete balanced design, and post hoc testing for pairwise differences was assessed using the Tukey honestly significant difference method. Reported *P* values are Tukey honestly significant difference–adjusted unless otherwise noted. In the model, conduit type was the fixed effect of interest, and valve internal diameter was considered a nuisance parameter addressed with a fixed effect.[34,35] Ordering effects were mitigated by the incomplete balance design.[34] Data are reported as model estimated mean±standard deviation (SD) or model estimated mean (95% confidence interval) unless otherwise noted with $P<0.05$ being considered statistically significant.

RESULTS

Hemodynamic Parameters

A summary of the valve, hemodynamic, and videometric characteristics of each conduit represented by marginal means with SDs is shown in the Table with the *P* value from the partial F-statistics for graft type from the fixed-effect model ANOVA for each outcome variable. Relative to native control aortic roots, the pressure and flow waveforms associated with each conduit type were all similar with no significant differences in any experimental grafts versus the control. After correcting for multiple comparisons, small statistically significant differences in mean arterial pressure (mean difference, SG–UG, 4.2±1.2, $P=0.04$), systolic pressure (mean difference, SG–UG, 4.5±1.4, $P=0.04$; control (C)–SG, 4.4±1.4, $P=0.04$; ACP–SG, –4.4±1.4,

 Circulation. 2020;142:1361–1373. DOI: 10.1161/CIRCULATIONAHA.120.046612

Table. Hemodynamic and Videometric Characteristics

	Control	ACP	Sm	Straight	Uni-Graft	Valsalva	*P* Value
Hemodynamic parameters							
Mean annular diameter, mm	27.0±1.4	27.0±1.4	27.0±1.4	27.0±1.4	27.0±1.4	27.0±1.4	…
Mean commissural height, mm	22.4±0.7	22.4±0.7	22.4±0.7	22.4±0.7	22.4±0.7	22.4±0.7	…
Mean cusp height, mm	17.0±0.7	17.0±0.7	17.0±0.7	17.0±0.7	17.0±0.7	17.0±0.7	…
Heart rate, bpm	70.0±0.0	70.0±0.0	70.0±0.0	70.0±0.0	70.0±0.0	70.0±0.0	…
Mean arterial pressure, mm Hg	100.2±0.7	98.9±1.7	99.1±2.0	102.9±4.3	98.7±3.2	101.7±2.0	0.02
Systolic blood pressure, mm Hg	117.5±1.0	117.5±2.1	117.9±2.6	121.9±4.3	117.4±3.4	120.9±2.2	<0.01
Diastolic blood pressure, mm Hg	84.5±1.1	81.6±1.5	82.2±1.7	85.4±4.3	82.1±2.9	84.5±2.4	0.04
Cardiac output, L/min	4.9±0.2	4.7±0.3	4.8±0.3	5.0±0.2	5.1±0.3	4.8±0.2	0.01
Effective stroke volume, mL	70.6±2.9	67.0±3.8	68.9±4.0	71.8±2.3	72.9±3.6	68.6±2.4	0.01
Pump stroke volume, mL	104.8±0.1	104.8±0.1	104.7±0.2	104.9±0.1	104.7±0.2	104.8±0.1	0.50
Mean transaortic pressure, mm Hg	4.2±2.2	8.5±3.4	9.0±4.0	10.9±2.9	15.7±7.8	9.3±3.4	<0.01
Effective orifice area, cm^2 (Gorlin)	2.9±0.4	2.3±0.4	2.2±0.4	2.0±0.2	1.7±0.4	2.1±0.3	<0.01
Regurgitant fraction, %	9.2±2.7	13.9±3.1	10.7±3.1	5.5±1.3	6.4±0.9	9.7±1.5	<0.01
Leakage rate, mL/s	–7.5±4.4	–16.2±5.0	–12.1±4.9	–4.8±2.1	–6.2±1.8	–10.7±2.5	<0.01
Leakage volume, mL	–3.6±2.3	–8.7±2.7	–6.5±2.7	–2.5±1.2	–3.3±1.0	–5.8±1.4	<0.01
Leakage energy loss, mJ	48.0±28.9	108.5±35.8	81.7±33.8	33.3±15.1	42.4±12.3	77.9±23.0	<0.01
Mean coronary flow, mL/min	237±25	236±24	232±19	246±25	243±24	238±28	0.74
Videometric analysis							
Peak root distensibility, %	12.9±2.5	10.3±2.8	8.1±2.6	3.1±1.2	11.8±5.0	10.0±2.3	<0.01
Left coronary cusp mean opening velocity, cm/s	22.9±1.3	34.2±4.4	34.8±5.9	28.1±3.2	32.0±1.9	31.2±3.0	<0.01
Right coronary cusp mean opening velocity, cm/s	24.9±3.5	36.1±4.4	32.1±5.4	29.2±3.7	32.7±2.9	32.1±3.4	<0.01
Noncoronary cusp mean opening velocity, cm/s	22.7±3.1	33.4±2.9	28.9±3.9	26.4±1.8	29.2±3.0	35.2±7.6	<0.01
Mean cusp opening velocity, cm/s	23.5±1.1	34.5±3.6	31.9±3.2	27.9±2.5	31.3±1.1	32.8±2.4	<0.01
Relative cusp opening force	1.0±0.0	1.7±0.5	1.7±0.3	1.2±0.2	1.3±0.2	1.6±0.2	<0.01
Left coronary cusp mean closing velocity, cm/s	–10.2±1.2	–15.8±2.5	–14.8±2.2	–10.5±1.4	–12.5±3.0	–14.8±1.1	<0.01
Right coronary cusp mean closing velocity, cm/s	–10.4±1.2	–15.2±2.1	–16.1±2.7	–9.2±0.7	–12.3±3.2	–14.8±2.8	<0.01
Noncoronary cusp mean closing velocity, cm/s	–7.9±0.9	–17.8±4.4	–15.8±0.7	–10.7±0.9	–11.6±1.8	–15.9±1.7	<0.01
Mean cusp closing velocity, cm/s	–9.5±0.8	–16.3±0.4	–15.5±0.6	–10.1±0.6	–12.1±1.5	–15.2±0.3	<0.01
Relative cusp closing force	1.0±0.0	8.5±2.7	7.0±3.9	1.8±0.3	4.1±1.3	5.8±1.7	<0.01

Data are presented as summarized marginal mean±SD in that they are unconditional over the experimental settings. The *P* values refer to partial *F* statistics for graft-type from the ANOVA for the given outcome's fixed-effect model. Note that the symbol "…" is used for *P* values for outcomes that are structurally deterministic. ACP indicates anticommissural plication; and Sm, Stanford modification.

P=0.04), and cardiac output (mean difference, ACP–UG, –0.4±0.1, *P*=0.01) were detected between various grafts. Based on an aggregate plot of pressure and flow tracings (Figure 5A and 5B), these differences were deemed clinically insignificant. Coronary blood mass flow rate did not differ between conduits significantly (Figure 5C, Data Supplement Table I), although we did not assess flow patterns or vortices. The shape of the UG ventricular pressure waveform differed from those of the other conduits and the control group with prolonged elevation of the ventricular pressure during systole before dropping back below mean aortic pressure. As a result, the mean transaortic pressure was significantly different between the groups (Figure 5D), with UGs having substantially higher mean transaortic gradients compared with the other conduits and control, with the exception of the SG group, which was also higher than the control group, though it did not differ when compared with the other grafts (Table II in the Data Supplement). Consequently, the effective orifice area was also significantly lower in the UG group, although all other conduits also exhibited

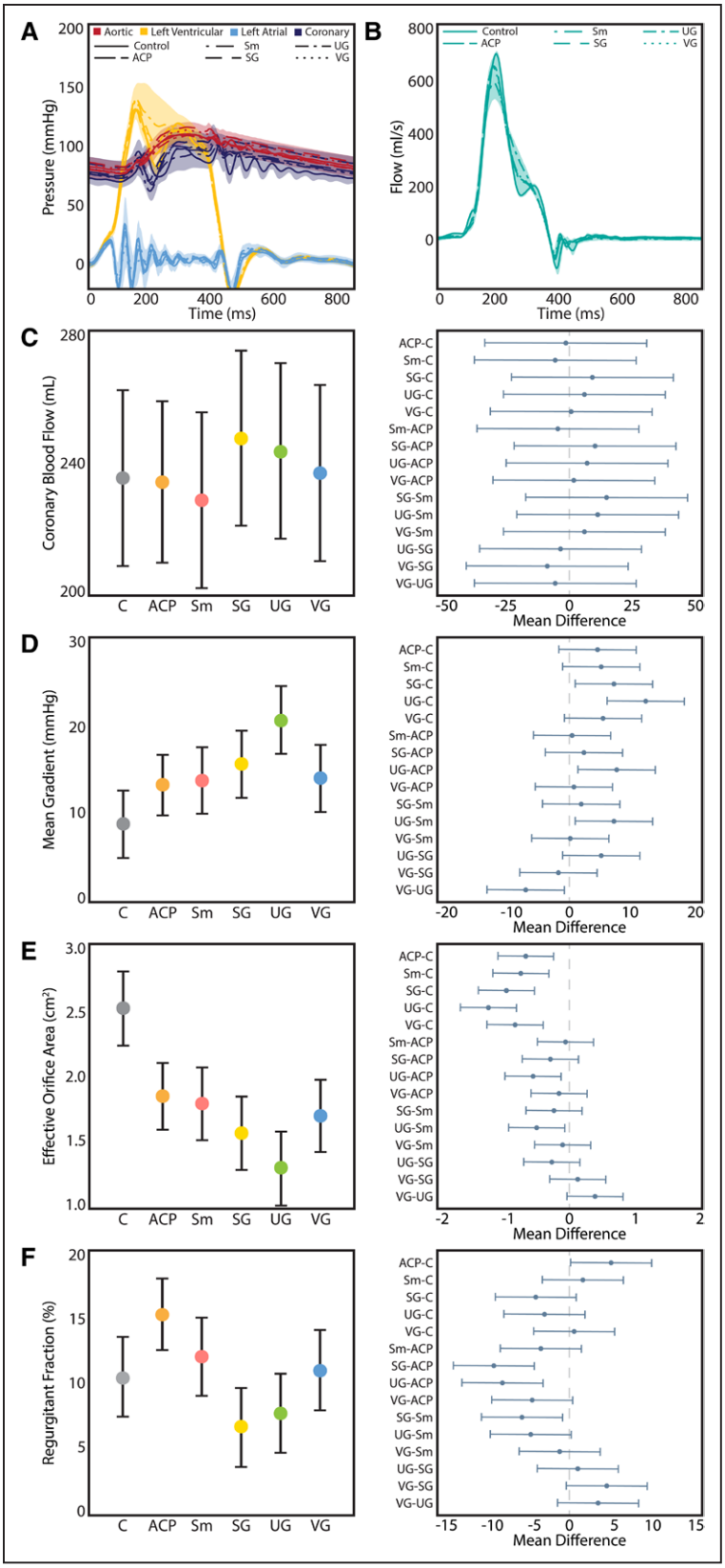

Figure 5. Hemodynamic parameters.
A, Composite pressure tracings between control and experimental grafts, with shaded regions representing the SDs. **B**, Composite flow waveforms between groups. Shaded regions represent SD. **C**, Coronary blood flow did not differ significantly between groups (P=0.74). **D**, Uni-Graft (UG) conduits were associated with a significantly higher mean gradient as compared with control (C), anticommissural plication (ACP), Stanford modification (Sm), and Valsalva graft (VG; Tukey adjusted P≤0.01, 0.01, 0.02, and 0.02, respectively). **E**, All of the grafts had significantly lower effective orifice areas than the control aortic roots (P<0.01 for each). The UG group had significantly smaller orifice areas than the ACP and Sm groups (P=0.01 and P=0.02, respectively). **F**, Regurgitant fraction varied considerably between groups (P<0.01), with straight graft (SG) and UG groups having the lowest regurgitant fractions. The ACP method resulted in a significantly higher regurgitant fraction vs the control group (15.1 [95% CI, 12.4–17.9] vs 10.4 [95% CI, 7.4–13.4], P=0.04), whereas the other methods resulted in similar regurgitant fractions vs the native control. For **C** through **F**, the left panel denotes model-adjusted means with 95% CIs, and the right panel displays Tukey-adjusted pairwise differences in means with 95% CIs. Reported P values are adjusted for multiple comparisons with Tukey correction.

significantly lower effective orifice areas compared with native aortic root controls (Figure 5E, Table III in the Data Supplement). Regurgitant fraction was also substantially different between the groups (Figure 5F, Table IV in the Data Supplement), with SG being significantly lower than ACP (P<0.01) and Sm (P=0.02), and trending toward being lower than VG (P=0.07); UG also had significantly lower regurgitant fractions

 Circulation. 2020;142:1361–1373. DOI: 10.1161/CIRCULATIONAHA.120.046612

than the ACP group (P<0.01). Interestingly, only ACP was found to have significantly higher regurgitant fractions than control roots (P=0.04), whereas the other conduits were not significantly different than the control after adjusting for multiple comparisons, though SG trended lower.

Videometric Analysis

High-speed videometric analysis was used to study graft deformation as well as leaflet biomechanics and kinematics. As expected, side-profile analysis demonstrated significantly lower peak root distensibility in the SG group versus the control and other conduits with the exception of Sm (Figure 6A, Movie I and Table V in the Data Supplement). The Sm trended toward lower root distensibility than the native aortic root, whereas ACP, UGs, and VGs had similar root distensibility to the control roots. Leaflet velocity analysis revealed that all grafts used in valve-sparing aortic root replacement except for SGs had significantly elevated cusp opening velocities versus the native control (P<0.01, Figure 6B, Table VI in the Data Supplement). As expected, the SG group did not have significantly different cusp opening forces versus control grafts, though it did result in significantly lower forces when compared with ACP (P=0.01), Sm (P=0.01), and VG (P=0.03) as shown in Figure 6C and Table VII in the Data Supplement. Interestingly, despite having significantly higher cusp opening velocities than the native control root because of the acceleration profile of the UG, relative opening forces were 1.6 (95% CI, 1.4–1.9) and not statistically significantly different than control roots (P=0.14), though UG did not significantly differ from other grafts. In terms of closing velocity, all conduit grafts apart from the SG resulted in significantly elevated cusp closing velocities versus native control aortic roots (P<0.01 for ACP–C, Sm–C, UG–C, and VG–C; Figure 6D, Table VIII in the Data Supplement). Control valves demonstrated a model estimated mean closing velocity of 9.1 cm/s (95% CI, 8.0–10.2), which was comparable to 9.7 cm/s (95% CI, 8.6–10.8) for the SG. Relative closing forces in the SG group were 1.4 (95% CI, –0.9 to 3.8), which was similar to native control roots (P=0.98) and UG (0.33), and significantly lower than the ACP relative closing force of 8.2 (95% CI, 6.1–10.3), Sm relative closing force of 6.6 (95% CI, 4.3–8.9), and VG relative closing force of 5.4 (95% CI, 3.1–7.7) as summarized in Figure 6E and Table IX in the Data Supplement. Again, despite having significantly higher closing velocities than the native control root because of the acceleration profile of the UG, relative closing forces of 3.8 (95% CI, 1.4–6.1) were not statistically significantly different than the control, though they trended toward being higher (P=0.1) and were only significantly lower than the ACP group (P=0.01).

DISCUSSION

In the 28 years since valve-sparing root replacement operations were first described, a tremendous amount of progress has been made in refining the techniques, evaluating clinical outcomes, and creating innovative new graft designs to further optimize this essential operation for patients. Valve-sparing aortic root replacement has been shown to have excellent long-term durability, with >90% freedom from reoperation using a variety of different approaches.[36–41] A multitude of studies have clearly demonstrated that the sinuses of Valsalva have a critical influence over the biomechanics of the aortic valve cusps, coronary blood flow, physiological helices within the ascending aorta, and cusp kinematics. Yet it is surprising that in this ex vivo counterbalanced and controlled crossover study, the SG most closely recapitulated the native aortic root.

All of the conduits tested had comparable gross hemodynamic performance to the native aortic root, along with similar mass coronary flow. We again found elevated leaflet velocities and forces in the VG, which we continue to attribute to spherical radial deformation of the commissures. A similar phenomenon is observed in the ACP technique and Sm, which both used a graft sized to the theoretical diameter of the sinuses, which is significantly larger than the native radial position of the commissures. Similar to what we observed in the VG group in our previous study,[18] these 2 conduit options resulted in higher regurgitant fractions than the SG group. Of note, the difference in regurgitant fraction between SG and VG was nearly significant in this study (P=0.07). It did not reach the level of significance seen in our previous study because of the loss in power secondary to multiple comparisons given that the observed values of regurgitant fraction in the SG and VG groups were consistent between studies. The Sm and VG were comparable with native roots in terms of regurgitant fraction, although both trended higher, whereas the ACP technique did exhibit a significantly higher regurgitant fraction versus the control. The reason for this, given that the Sm and ACP techniques both used a size 36 graft (and the VG skirt diameter is also 36 mm), is unclear. It is possible that the effect of reconstructing the 3-dimensional shape of the annulus does not have its intended effect in the ex vivo model given that the LVOT is only partially recreated to match its native material properties, and the elastomeric sewing ring only allows for more natural passive motion and not the dynamic contraction and relaxation seen in vivo, which is a limitation. In addition, although the aortomitral continuity is recreated to some degree in terms of maintaining the anatomic angle between the aortic and mitral valve, the 2 valves are physically separated in our model for isolated study.

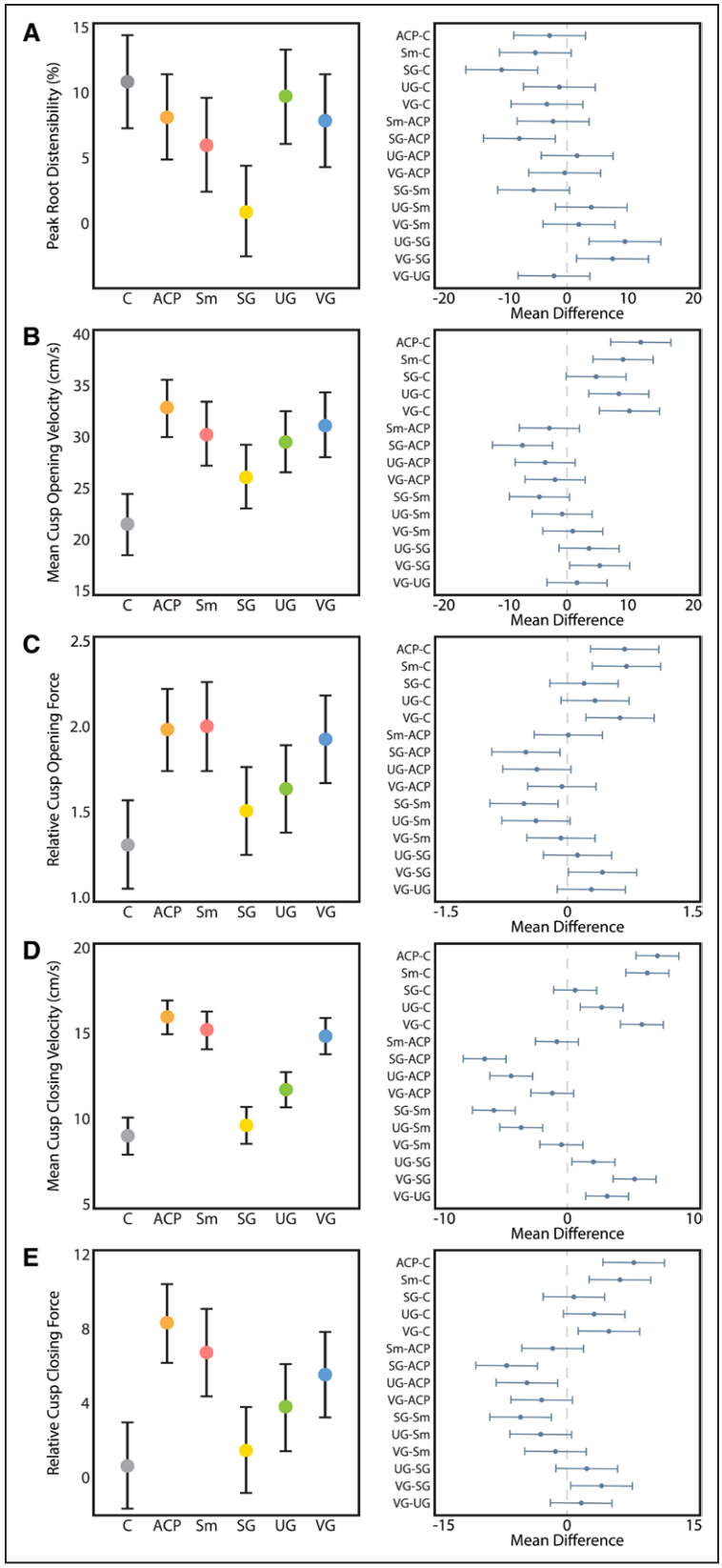

Figure 6. Videometric parameters.
A, Peak aortic root distensibility trended lower in the grafts vs the control but was only statistically significantly lower in the straight graft group (Tukey adjusted $P \leq 0.01$), with the straight graft being significantly lower than all grafts ($P \leq 0.01$ for each) with the exception of Stanford modification (Sm). **B**, All grafts except straight graft (SG) had significantly higher mean cusp opening velocity than native aortic root controls ($P < 0.01$ for each). **C**, Relative cusp opening forces were similar between the SG, Uni-Graft (UG), and control (C) groups, whereas the anticommissural plication (ACP), Sm, and Valsalva graft (VG) groups had significantly higher relative cusp opening forces ($P \leq 0.01$ for each). The SG group experienced significantly lower relative opening forces than the ACP, Sm, and VG groups (Tukey adjusted $P = 0.01$, 0.01, and 0.03, respectively). **D**, Closing velocity was significantly higher than in the native root in all grafts except for the SG group ($P < 0.01$ for each). The SG group had significantly lower closing velocities vs any other conduit ($P \leq 0.01$ for each comparison). The UG group had significantly lower closing velocities than the ACP, Sm, and VG groups ($P \leq 0.01$ for each). **E**, Only the SG and UG groups experienced relative closing forces approaching that of the native root, whereas relative forces were >5-fold higher in the ACP, Sm, UG, and VG groups ($P \leq 0.01$ for each). Left panels report model-adjusted means with 95% CIs, and right panels display Tukey-adjusted pairwise differences in means with 95% CIs. Reported *P* values are adjusted for multiple comparisons with Tukey correction.

Other limitations include that we used porcine and not human valves, which differ in some ways. Overall cusp height is similar between humans and pigs, but relative cusp sizes do vary, with pigs having a larger right cusp and smaller noncoronary cusp.[42–44] It is possible, though unlikely, that this difference interacts in such a way to change overall root biomechanics. In addition, we did not evaluate flow profiles, only leaflet velocimetry

and mass flow rates, and our study does not replicate systemic effects found in the body, the complex helical flow patterns generated by the left ventricle, or the non-Newtonian effects of blood. Clinically, many patients undergoing valve-sparing root replacement have some degree of aortic insufficiency and distortion or dilation of their aortic root, whereas in our study the porcine valves were anatomically normal. Baseline aortic root disease may influence conduit choice, and this has not been evaluated in our current study. We are in the process of obtaining diseased specimens for study in future experiments; however, obtaining a sufficient number of diseased aortic roots is time-consuming given their scarcity. In clinical practice, we are guided by long-term outcomes, whereas in this study, we gathered short-term biomechanical data. Gathering long-term data is important; however, demonstrating and discovering differences in kinematic dynamics and outcomes, even in the short term, provide an empirical basis for designing future experiments and clinical studies of long-term outcomes. These biomechanical findings will guide not only future studies but also future innovations as we develop more refined materials and techniques to recreate the native aortic root. Despite these limitations, our ex vivo model does allow for a controlled and reproducible evaluation of multiple surgical options on the same specimen, which would be impossible in clinical studies.

Based on our initial hypotheses behind why neosinus reconstruction with the VG does not have its intended effect on cusp kinematics, we expected the UG to mostly closely match the native aortic root given that it possesses sinuses but also maintains the cylindrical conformation of the aortic commissures. Indeed, this graft does result in a low regurgitant fraction, and it also demonstrates physiological root distensibility comparable with that of the control root in that the sinuses expand but the commissural position is maintained. Curiously, we observed elevated opening and closing velocities in the UG group, despite this graft maintaining the cylindrical position of the commissures. More interesting, however, the UG's acceleration profile mitigated the effects of these higher velocities on force outcomes, suggesting that although radial commissural displacement likely influences cusp velocities, there are likely additional nuanced factors at play. It appears that as designed, the distensibility of this graft and sinus shape to some degree did attenuate the forces present within the root, similar to what the native elastic root achieves. However, the UG resulted in high mean transaortic gradients with a comparable reduction in effective orifice area, which could potentially be mitigated by upsizing the graft, though what effect this has on leaflet kinematics is unclear. Unfortunately, the UG is not commercially available in the United States.

Despite being the conduit that least resembles the native aortic root, the SG performed most closely to the native aortic root with regards to cusp velocity and relative cusp forces. The SG did have higher transaortic gradients than control roots, as well as smaller effective orifice areas than control roots, but these were comparable with the range observed with the other grafts. Although the SG did maintain cylindrical commissural position, it had little root distensibility and was relatively inelastic in the transverse dimension. Despite this, closing velocities and relative forces were lowest in this conduit. Other benefits of the SG include that it is widely available throughout the world from multiple manufacturers and has a lower cost relative to conduit options using novel graft designs, larger grafts, or multiple grafts. The SG is also the most simplistic of the available conduits, which, combined with its inelasticity, may make this conduit more forgiving in terms of reliably and reproducibly performing the reimplantation procedure. These features, combined with the available, albeit limited, clinical data, make the SG our preferred conduit for performing this operation.

Conclusions

Through the use of a novel ex vivo model of valve-sparing aortic root replacement with an incomplete counterbalanced repeated measures design, we comprehensively examined the biomechanical differences in all clinically available conduits that can be used for this operation. Surprisingly, the SG, which makes no attempt to mimic native aortic root neosinuses, appears to perform most closely to the native aortic root in terms of cusp velocity and forces, which could potentially result in less wear on the valve cusps and result in superior clinical durability over conduits with higher cusp velocities and forces. Although it is likely that the biomechanical properties of conduits have clinical ramifications, further study is required and is currently underway using ovine and porcine large animal models of valve-sparing aortic root replacement, examining the influence conduit choice has on flow dynamics with 4-dimensional magnetic resonance imaging. Overall, the valve-sparing aortic root replacement operation is highly effective and durable regardless of conduit. To improve on this further and more closely mimic nature, however, we may have to look beyond simply geometry as other elements are clearly important in this complex anatomic structure.

ARTICLE INFORMATION

Received March 1, 2020; accepted August 26, 2020.

This manuscript was sent to Marc Ruel, Cardiovascular Surgery Issue Editor, for review by expert referees, editorial decision, and final disposition.

The Data Supplement is available with this article at https://www.ahajournals.org/doi/suppl/10.1161/CIRCULATIONAHA.120.046612.

ORIGINAL RESEARCH ARTICLE

Correspondence

Y. Joseph Woo, MD, Department of Cardiothoracic Surgery, Department of Bioengineering, Stanford University, Falk Cardiovascular Research Building CV-235, 300 Pasteur Drive, Stanford, CA 94305-5407. Email joswoo@stanford.edu

Affiliations

Department of Cardiothoracic Surgery (M.J.P., A.M.I.-M., M.B., H.W., C.E.H., H.J.L., J.M.F., A.D.T., Y.Z., M.M., J.W.M., Y.J.W.), Department of Mechanical Engineering (A.M.I.M.), Department of Health Research and Policy (M.B.), Department of Bioengineering (Y.J.W.), Stanford University, CA.

Acknowledgments

An abstract based on this manuscript was presented at the 2019 AHA Scientific Sessions and won the Vivien Thomas Young Investigator Award. The authors thank the Rittenberg Family Foundation for their generous support of this research.

Sources of Funding

This work was supported by the National Institutes of Health (grant numbers R01HL152155 and R01HL089315-01 to Dr Woo), the American Heart Association (17POST33410497 to Dr Paulsen, 18POST33990223 to Dr Wang, by the National Science Foundation (GRFP DGE-1656518 to A.M. Imbrie-Moore), and by the Stanford Graduate Fellowship in Science and Engineering (to A.M. Imbrie-Moore).

Disclosures

None.

Supplemental Materials

Data Supplement Tables I–IX
Data Supplement Movie I

REFERENCES

1. David TE, Feindel CM. An aortic valve-sparing operation for patients with aortic incompetence and aneurysm of the ascending aorta. *J Thorac Cardiovasc Surg.* 1992;103:617–21; discussion 622.
2. Sarsam MA, Yacoub M. Remodeling of the aortic valve anulus. *J Thorac Cardiovasc Surg.* 1993;105:435–438.
3. Lenoir M, Maesen B, Stevens LM, Cartier R, Demers P, Poirier N, Tousch M, El-Hamamsy I. Reimplantation versus remodelling with ring annuloplasty: comparison of mid-term outcomes after valve-sparing aortic root replacement. *Eur J Cardiothorac Surg.* 2018;54:48–54. doi: 10.1093/ejcts/ezy016
4. Leyh RG, Schmidtke C, Sievers HH, Yacoub MH. Opening and closing characteristics of the aortic valve after different types of valve-preserving surgery. *Circulation.* 1999;100:2153–2160. doi: 10.1161/01.cir.100.21.2153
5. Bechsgaard T, Lindskow T, Lading T, Røpcke DM, Nygaard H, Johansen P, Nielsen SL, Hasenkam JM. Biomechanical characterization and comparison of different aortic root surgical techniques. *Interact Cardiovasc Thorac Surg.* 2019;28:112–119. doi: 10.1093/icvts/ivy187
6. De Paulis R, Scaffa R, Salica A, Weltert L, Wolf LG, Folino G. Aortic valve sparing techniques: pearls and pitfalls. *J Vis Surg.* 2019;5:74–74.
7. David TE, Feindel CM, Webb GD, Colman JM, Armstrong S, Maganti M. Long-term results of aortic valve-sparing operations for aortic root aneurysm. *J Thorac Cardiovasc Surg.* 2006;132:347–354. doi: 10.1016/j.jtcvs.2006.03.053
8. Liu L, Wang W, Wang X, Tian C, Meng YH, Chang Q. Reimplantation versus remodeling: a meta-analysis. *J Card Surg.* 2011;26:82–87. doi: 10.1111/j.1540-8191.2010.01171.x
9. Salica A, Pisani G, Morbiducci U, Scaffa R, Massai D, Audenino A, Weltert L, Guerrieri Wolf L, De Paulis R. The combined role of sinuses of Valsalva and flow pulsatility improves energy loss of the aortic valve. *Eur J Cardiothorac Surg.* 2016;49:1222–1227. doi: 10.1093/ejcts/ezv311
10. Galea N, Piatti F, Sturla F, Weinsaft JW, Lau C, Chirichilli I, Carbone I, Votta E, Catalano C, De Paulis R, et al; Cornell International Consortium for Aortic Surgery (CICAS). Novel insights by 4D Flow imaging on aortic flow physiology after valve-sparing root replacement with or without neosinuses. *Interact Cardiovasc Thorac Surg.* 2018;26:957–964. doi: 10.1093/icvts/ivx431
11. Galea N, Piatti F, Lau C, Sturla F, Weltert L, Carbone I, De Paulis R, Gaudino M, Girardi LN; Cornell International Consortium for Aortic Surgery (CICAS). 4D flow characterization of aortic blood flow after valve sparing root reimplantation procedure. *J Vis Surg.* 2018;4:95. doi: 10.21037/jovs.2018.03.17
12. Gaudino M, Piatti F, Lau C, Sturla F, Weinsaft JW, Weltert L, Votta E, Galea N, Chirichilli I, Di Franco A, et al. Aortic flow after valve sparing root replacement with or without neosinuses reconstruction. *J Thorac Cardiovasc Surg.* 2019;157:455–465. doi: 10.1016/j.jtcvs.2018.06.094
13. Kvitting JP, Ebbers T, Wigström L, Engvall J, Olin CL, Bolger AF. Flow patterns in the aortic root and the aorta studied with time-resolved, 3-dimensional, phase-contrast magnetic resonance imaging: implications for aortic valve-sparing surgery. *J Thorac Cardiovasc Surg.* 2004;127:1602–1607. doi: 10.1016/j.jtcvs.2003.10.042
14. Bellhouse BJ, Bellhouse FH, Reid KG. Fluid mechanics of the aortic root with application to coronary flow. *Nature.* 1968;219:1059–1061. doi: 10.1038/2191059a0
15. Grande-Allen KJ, Cochran RP, Reinhall PG, Kunzelman KS. Re-creation of sinuses is important for sparing the aortic valve: a finite element study. *J Thorac Cardiovasc Surg.* 2000;119(4 Pt 1):753–763. doi: 10.1016/S0022-5223(00)70011-0
16. Thubrikar MJ, Nolan SP, Aouad J, Deck JD. Stress sharing between the sinus and leaflets of canine aortic valve. *Ann Thorac Surg.* 1986;42:434–440. doi: 10.1016/s0003-4975(10)60554-1
17. Beckmann E, Leone A, Martens A, Mariani C, Krueger H, Cebotari S, Di Bartolomeo R, Haverich A, Shrestha ML, Pacini D. Comparison of two strategies for aortic valve-sparing root replacement. *Ann Thorac Surg.* 2020;109:505–511. doi: 10.1016/j.athoracsur.2019.07.006
18. Paulsen MJ, Kasinpila P, Imbrie-Moore AM, Wang H, Hironaka CE, Koyano TK, Fong R, Chiu P, Goldstone AB, Steele AN, et al. Modeling conduit choice for valve-sparing aortic root replacement on biomechanics with a 3-dimensional-printed heart simulator. *J Thorac Cardiovasc Surg.* 2019;158:392–403. doi: 10.1016/j.jtcvs.2018.10.145
19. Gleason TG. New graft formulation and modification of the David reimplantation technique. *J Thorac Cardiovasc Surg.* 2005;130:601–603. doi: 10.1016/j.jtcvs.2005.02.016
20. Swanson M, Clark RE. Dimensions and geometric relationships of the human aortic valve as a function of pressure. *Circ Res.* 1974;35:871–882. doi: 10.1161/01.res.35.6.871
21. Markl M, Draney MT, Miller DC, Levin JM, Williamson EE, Pelc NJ, Liang DH, Herfkens RJ. Time-resolved three-dimensional magnetic resonance velocity mapping of aortic flow in healthy volunteers and patients after valve-sparing aortic root replacement. *J Thorac Cardiovasc Surg.* 2005;130:456–463. doi: 10.1016/j.jtcvs.2004.08.056
22. Demers P, Miller DC. Simple modification of "T. David-V" valve-sparing aortic root replacement to create graft pseudosinuses. *Ann Thorac Surg.* 2004;78:1479–1481. doi: 10.1016/j.athoracsur.2003.08.032
23. Richardt D, Karluss A, Schmidtke C, Sievers HH, Scharfschwerdt M. A new sinus prosthesis for aortic valve-sparing surgery maintaining the shape of the root at systemic pressure. *Ann Thorac Surg.* 2010;89:943–946. doi: 10.1016/j.athoracsur.2009.10.066
24. Schmidtke C, Sievers HH, Frydrychowicz A, Petersen M, Scharfschwerdt M, Karluss A, Stierle U, Richardt D. First clinical results with the new sinus prosthesis used for valve-sparing aortic root replacement. *Eur J Cardiothorac Surg.* 2013;43:585–590. doi: 10.1093/ejcts/ezs318
25. De Paulis R, De Matteis GM, Nardi P, Scaffa R, Buratta MM, Chiariello L. Opening and closing characteristics of the aortic valve after valve-sparing procedures using a new aortic root conduit. *Ann Thorac Surg.* 2001;72:487–494. doi: 10.1016/s0003-4975(01)02747-3
26. De Paulis R, De Matteis GM, Nardi P, Scaffa R, Bassano C, Chiariello L. Analysis of valve motion after the reimplantation type of valve-sparing procedure (David I) with a new aortic root conduit. *Ann Thorac Surg.* 2002;74:53–57. doi: 10.1016/s0003-4975(02)03583-x
27. David TE, Armstrong S, Ivanov J, Feindel CM, Omran A, Webb G. Results of aortic valve-sparing operations. *J Thorac Cardiovasc Surg.* 2001;122:39–46. doi: 10.1067/mtc.2001.112935
28. Miller DC. Valve-sparing aortic root replacement in patients with the Marfan syndrome. *J Thorac Cardiovasc Surg.* 2003;125:773–778. doi: 10.1067/mtc.2003.162
29. Paulsen MJ, Bae JH, Imbrie-Moore AM, Wang H, Hironaka CE, Farry JM, Lucian H, Thakore AD, Cutkosky MR, Woo YJ. Development and ex vivo validation of novel force-sensing neochordae for measuring chordae tendineae tension in the mitral valve apparatus

using optical fibers with embedded Bragg gratings. *J Biomech Eng*. 2020;142:0145011-0145019.
30. Imbrie-Moore AM, Paulsen MJ, Thakore AD, Wang H, Hironaka CE, Lucian HJ, Farry JM, Edwards BB, Bae JH, Cutkosky MR, et al. Ex vivo biomechanical study of apical versus papillary neochord anchoring for mitral regurgitation. *Ann Thorac Surg*. 2019;108:90–97. doi: 10.1016/j.athoracsur.2019.01.053
31. Paulsen MJ, Imbrie-Moore AM, Wang H, Bae JH, Hironaka CE, Farry JM, Lucian HJ, Thakore AD, MacArthur JW, Cutkosky MR, et al. Mitral chordae tendineae force profile characterization using a posterior ventricular anchoring neochordal repair model for mitral regurgitation in a three-dimensional-printed ex vivo left heart simulator. *Eur J Cardiothorac Surg*. 2020;57:535–544. doi: 10.1093/ejcts/ezz258
32. Imbrie-Moore AM, Paullin CC, Paulsen MJ, Grady F, Wang H, Hironaka CE, Farry JM, Lucian HJ, Woo YJ. A novel 3D-printed preferential posterior mitral annular dilation device delineates regurgitation onset threshold in an ex vivo heart simulator. *Med Eng Phys*. 2020;77:10–18. doi: 10.1016/j.medengphy.2020.01.005
33. Imbrie-Moore AM, Paulsen MJ, Zhu Y, Wang H, Lucian HJ, Farry JM, MacArthur JW, Ma M, Woo YJ. A novel cross-species model of Barlow's disease to biomechanically analyze repair techniques in an ex vivo left heart simulator. *J Thorac Cardiovasc Surg*. 2020. In press. doi: 10.1016/j.jtcvs.2020.01.086
34. Yandell BS. *Practical Data Analysis for Designed Experiments (Chapman & Hall/crc Texts in Statistical Science)*. London: Chapman and Hall/crc; 1997.
35. Miller RG. *Simultaneous Statistical Inference*. New York, NY: Springer New York; 1981.
36. Price J, Magruder JT, Young A, Grimm JC, Patel ND, Alejo D, Dietz HC, Vricella LA, Cameron DE. Long-term outcomes of aortic root operations for Marfan syndrome: a comparison of Bentall versus aortic valve-sparing procedures. *J Thorac Cardiovasc Surg*. 2016;151:330–336. doi: 10.1016/j.jtcvs.2015.10.068
37. David TE, David CM, Feindel CM, Manlhiot C. Reimplantation of the aortic valve at 20 years. *J Thorac Cardiovasc Surg*. 2017;153:232–238. doi: 10.1016/j.jtcvs.2016.10.081
38. David TE, Feindel CM, David CM, Manlhiot C. A quarter of a century of experience with aortic valve-sparing operations. *J Thorac Cardiovasc Surg*. 2014;148:872–9; discussion 879. doi: 10.1016/j.jtcvs.2014.04.048
39. Gaudino M, Weltert L, Munjal M, Lau C, Elsayed M, Salica A, Gambardella I, Mills E, De Paulis R, Girardi LN; Cornell International Consortium for Aortic Surgery (CICAS). Early clinical outcome after aortic root replacement using a biological composite valved graft with and without neo-sinuses. *Eur J Cardiothorac Surg*. 2017;51:316–321. doi: 10.1093/ejcts/ezw253
40. De Paulis R, Chirichilli I, Scaffa R, Weltert L, Maselli D, Salica A, Guerrieri Wolf L, Bellisario A, Chiariello L. Long-term results of the valve reimplantation technique using a graft with sinuses. *J Thorac Cardiovasc Surg*. 2016;151:112–119. doi: 10.1016/j.jtcvs.2015.08.026
41. Miller DC. Rationale and results of the Stanford modification of the David V reimplantation technique for valve-sparing aortic root replacement. *J Thorac Cardiovasc Surg*. 2015;149:112–114. doi: 10.1016/j.jtcvs.2014.08.077
42. Sim EK, Muskawad S, Lim CS, Yeo JH, Lim KH, Grignani RT, Durrani A, Lau G, Duran C. Comparison of human and porcine aortic valves. *Clin Anat*. 2003;16:193–196. doi: 10.1002/ca.10149
43. Sands MP, Rittenhouse EA, Mohri H, Merendino KA. An anatomical comparison of human pig, calf, and sheep aortic valves. *Ann Thorac Surg*. 1969;8:407–414. doi: 10.1016/s0003-4975(10)66071-7
44. Wang C, Lachat M, Regar E, von Segesser LK, Maisano F, Ferrari E. Suitability of the porcine aortic model for transcatheter aortic root repair. *Interact Cardiovasc Thorac Surg*. 2018;26:1002–1008. doi: 10.1093/icvts/ivx381